Theme V – Models and Techniques for Analyzing Seismicity

Seismicity Rate Changes

David Marsan[1] • Max Wyss[2]

1. Institut des Sciences de la Terre, CNRS, Universite de Savoie
2. World Agency of Planetary Monitoring and Earthquake Risk Reduction

How to cite this article:

Marsan, D., and M. Wyss (2011), Seismicity rate changes, Community Online Resource for Statistical Seismicity Analysis, doi:10.5078/corssa-25837590. Available at http://www.corssa.org.

Document Information:

Issue date: 30 January 2011 Version: 1.0

Contents

Abstract Earthquake time series can be characterized by the rate of occurrence, which gives the number of earthquakes per unit time. Occurrence rates generally evolve through time; they strongly increase immediately after a large shock, for example. Understanding and modeling this time evolution is a fundamental issue in seismology, and more particularly for prediction purposes.

Seismicity rate changes can be subtle, with a slow time evolution, or with a gradual onset long after the cause. Therefore, it has proved problematic in many instances to assess whether a change in rate is real, i.e., whether it is statistically significant, or not. We here review and describe existing methods developed for measuring seismicity rate changes, and for testing the significance of these changes. Null hypotheses of 'no change' are formulated, that depend on the context. Statistics are then defined to quantify the departure from this null hypothesis. We illustrate these methods with several examples.

1 Why compute seismicity rate changes?

Earthquakes, especially of small to moderate sizes, are generally abundant in active fault zones. Although they do not matter in terms of seismic hazard, their occurrences are a signature of the state of the crust at seismogenic depths, that cannot otherwise be probed or subject to direct measurements. As such, they provide an unique source of information regarding to the mechanical state of potentially dangerous seismic asperities.

Changes in seismicity patterns are therefore likely to be correlated to changes in stress, as evidenced by aftershock sequences, or by more subtle seismicity dynamics caused by nucleation processes of large earthquakes. A key issue is then to quantify changes in the rate of earthquake occurrences, in particular by checking whether such changes are actually statistically significant or not. In many applications the change in rate is obvious, and does not really require any specific analysis; this is clearly the case when considering the whole rupture area of a given mainshock, for which the increase in rate is always extremely significant. However, more demanding analyses are needed when inspecting areas that only experience a weak or mild aftershock triggering, as is the case far off the main fault, or for small areas close to the fault that are thought of as undergoing stress unloading (eg, stress shadows). Quantitative measures of a change in seismicity are more particularly required when trying to detect specific patterns (eg, relative quiescence) prior to large shocks, as an attempt to identify precursory phenomena that could be used for earthquake prediction strategies.

2 Prerequisite

The reader should be familiar with Poisson processes (Theme III) and seismicity models (Theme V), at least for the nonstationary treatment of section 5, before reading this article.

We will assume throughout this chapter that the earthquake data have been quality-controlled, in particular that a magnitude of completeness m_c has been estimated, that only earthquakes with magnitudes greater than this m_c are kept, and that the magnitudes are all computed in a consistent way. We refer the reader to *Habermann* (1987) for a review on how spurious seismicity rate changes can arise from artificial effects. Such effects can be detected by considering separate rate changes for various magnitude bands. We will here only investigate rate changes for the whole magnitude interval $m \geq m_c$.

3 An introductory case study

We start by studying the changes in earthquake activity remotely caused by the Landers earthquake, as reported in *Hill et al.* (1993). The number of earthquakes that occurred at several remarkable locations, in the seven days prior to and in the seven days following Landers, are summarized in Table 1 (this is only an excerpt of Table 1 of *Hill et al.* (1993)):

Region	N_b	N_a
Death Valley	6	11
White Mountains	0	27
Parkfield	8	11
Mono Basin	3	12
Geysers	70	60

Table 1 Number of earthquakes seven days before (N_b) and after (N_a) the Landers earthquake, in 5 selected regions. Taken from *Hill et al.* (1993).

It is clear from these numbers that the White Mountains region experienced a significant increase of activity after Landers. The four other regions were however not so much influenced by it. We now define a measure that can tell us how much confident we can be in arguing a change has occurred. We will develop our calculations with the Death Valley region, and eventually will give the results for all 5 regions.

To begin with, it is important to emphasize that a change in *number* from $N_b = 6$ to $N_a = 11$ does not necessarily imply that the underlying seismicity *rate* indeed increased. These numbers are outcomes of a Poisson process, very much like the number of clients entering the local bakery during a 5 minute interval. We could

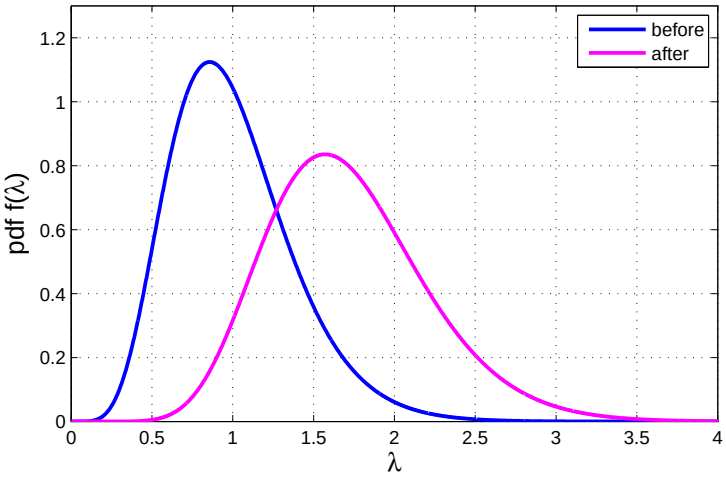

Fig. 1 Probability density function of the earthquake rate (in 1/day) observed at Death Valley, 7 days before and 7 days after the 1992 Landers earthquake

very well observe that 6 clients came between 11:20 and 11:25, while 11 came between 11:25 and 11:30, without necessarily conclude that the second interval is on ensemble average nearly twice as busy as the first. Actually, the chance is that the two intervals are in general equivalent, but today, by pure luck, it happened that $N_b = 6$ and $N_a = 11$. A null hypothesis could be formulated: the numbers N_a and N_b are drawn from two independent, identically distributed Poisson laws, i.e., the two intervals are equally busy, and the rate of clients per minute is $\frac{6+11}{10} = 1.7$. Then the chance of observing $N_b = 6$ and $N_a = 11$ is $P(N_b = 6, N_a = 11) = e^{-17} \times \frac{8.5^6}{6!} \times \frac{8.5^{11}}{11!} = 0.91\%$. This combination of outcomes will therefore occur 0.43 times per day on average, counting 8 business hours per day, so that our observing it is quite plausible.

We further develop this argument. For any given region, we denote by λ_b and λ_a the earthquake rates before and after Landers. As explained in the previous paragraph, these rates are unknown: for example, one could intuitively argue that the 6 earthquakes observed at Death Valley in the week prior to Landers could reasonably be due to a daily rate λ_b in the $[\frac{1}{7}, 3]$ day^{-1} range, at the time scale of 1 week. Indeed, the probability to have 6 occurrences in 7 days if $\lambda_b = \frac{1}{7}$ day^{-1} amounts to $P(N_b = 6|\lambda_b = \frac{1}{7}) = e^{-1}\frac{1^6}{6!} = 5.1 \times 10^{-4}$; equivalently, $P(N_b = 6|\lambda_b = 3) = e^{-21}\frac{21^6}{6!} = 9 \times 10^{-5}$, while it becomes at max $P(N_b = 6|\lambda_b = \frac{6}{7}) = e^{-6}\frac{6^6}{6!} = 0.161$. The probability density function associated with the rate λ for N earthquakes occurring in a time interval Δt is

$$f(\lambda) \;=\; \Delta t \; e^{-\lambda \Delta t} \frac{(\lambda \Delta t)^N}{N!} \tag{1}$$

We show in Figure 1 the two pdf (before and after Landers) for Death Valley. The maximum likelihood is given by $\lambda = \frac{N}{\Delta t}$. Using these pdf, we can compute the probability that the earthquake rate increased by more than a given ratio r, i.e.,

$$P\left(\frac{\lambda_a}{\lambda_b} > r\right) = \int_0^\infty d\lambda_b \; f_b(\lambda_b) \int_{r\lambda_b}^\infty d\lambda_a \; f_a(\lambda_a) \tag{2}$$

This yields

$$P\left(\frac{\lambda_a}{\lambda_b} > r\right) = 1 - \frac{1}{N_a!\; N_b!} \int_0^\infty dx \; e^{-x} \; x^{N_b} \; \Gamma(N_a + 1, rx) \tag{3}$$

where $\Gamma(n, x) = \int_0^x dt \; e^{-t} \; t^{n-1}$ is the incomplete Gamma function. This can be further generalized to the case where the two time intervals 'before' and 'after' do not have the same durations: the last term of Equation 3 must then be changed to $\Gamma\left(N_a + 1, rx\frac{\Delta t_a}{\Delta t_b}\right)$.

This expression can only be solved numerically. A Matlab program that does this is given by:

```
function P=probability_increase(r,Nb,Na,Dtb,Dta)
% estimate the probability that the rate of earthquakes
% 'after' is at least r times greater than the rate of
% earthquakes 'before'. Nb earthquakes are observed in a time
% duration Dtb before, and Na in Dta after.

if(Nb<25) Nm=max([10 10*Nb]); x=0:Nm*10^(-3):Nm;
else x=Nb-5*sqrt(Nb):sqrt(Nb)*10^(-2):Nb+5*sqrt(Nb); end

tmp=Nb*log(x); if(Nb==0 & x(1)==0) tmp(1)=0; end
tmp=tmp-x-gammaln(Nb+1)+log(gammainc(r*Dta/Dtb*x,Na+1))+log((x(2)-x(1)));
P=1-sum(exp(tmp));
```

Applying this to the Death Valley case, we find that the probability for an increase of seismicity ($r = 1$) is $P\left(\frac{\lambda_a}{\lambda_b} > 1\right) = 0.881$. The probability for a two-fold increase ($r = 2$) is $P\left(\frac{\lambda_a}{\lambda_b} > 2\right) = 0.391$. The decay of this probability with r is shown in Figure 2.

From these curves, it is easy to determine the 90% confidence interval for r, that is, the interval $r_1 < r < r_2$ so that $P(r_1) = 5\%$ and $P(r_2) = 95\%$. We here find $0.80 < r < 4.02$. Similarly, the 99% confidence interval is $0.52 < r < 6.79$. In both cases, r values less than 1 are a possibility, as could have been guessed by direct

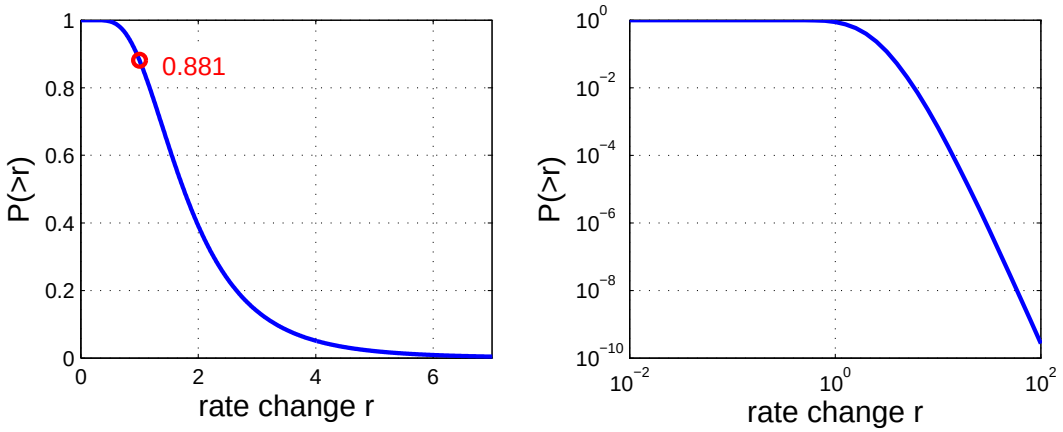

Fig. 2 Probability of a change in seismicity rate greater than ratio r, for the Death Valley region, in linear and log-log scales.

inspection of Figure 2. We therefore cannot be confident that the Death Valley region really experienced an increase in seismicity rate after the Landers earthquake, at least at the time scale of one week.

Equivalently, it is interesting to compute the number of earthquakes that should have occurred in the week following Landers and that would have resulted in $P\left(\frac{\lambda_a}{\lambda_b} > 1\right)$ being greater than a threshold value p. For $p = 0.90$, we would have needed at least 12 earthquakes (only one more than the 11 actually observed), while for $p = 0.99$ this number goes up to 18.

We summarize in Table 2 the results for the five regions. Only the White Mountains and the Mono Basin regions can be considered with good confidence (greater than 98% in both cases) as having undergone an increase in seismicity rate.

region	$r = 1$	$r = 2$	$r = 5$
Death Valley	0.88	0.39	0.02
White Mountains	1.00	1.00	0.93
Parkfield	0.75	0.19	0.0028
Mono Basin	0.989	0.83	0.27
Geysers	0.19	7×10^{-7}	2×10^{-10}

Table 2 Probability $P\left(\frac{\lambda_a}{\lambda_b} > r\right)$ for three values of r, for the 5 regions as in Table 1.

4 Measuring the significance of a seismicity rate change

We now introduce several statistics that have been or could be proposed to measure the significance of seismicity rate changes. We keep the same notations as above: *before* time T of interest (eg, time of occurrence of the Landers mainshock), N_b earthquakes were observed to occur in a time interval of duration Δt_b, while *after* T, we observe N_a earthquakes in a time Δt_a. The question is still the same: how significant is the rate change that occurred at T, if any? The corresponding null hypothesis is that there was no change, i.e., *before* and *after* are characterized by the same Poisson process with the same mean rate λ.

4.1 Statistics $\mathcal{P}$ and γ (*Marsan and Nalbant* 2005)

The probability $\mathcal{P} = P\left(\frac{\lambda_a}{\lambda_b} > 1\right)$ that $\lambda_a > \lambda_b$, is a good and simple measure of how the two processes characterizing *before* and *after* differ of each other. We first discuss the case when $\Delta t_a = \Delta t_b$, for simplicity. It is easy to show in this case that $\mathcal{P} = 0.5$ when $N_a = N_b$: there is as much chance that activation ($r > 1$) or inhibition ($r < 1$) took place if we observe the same numbers of earthquakes before and after T. This value $\mathcal{P} = 0.5$ corresponds to the maximum overlap between the two pdf of λ_a and λ_b. Departure from $\lambda_a = \lambda_b$ will therefore result in $\mathcal{P}$ departing from 0.5, and going towards either 0 if there is a shutdown of activity, or 1 if there is activation.

Remarkably, in the null hypothesis $\lambda_a = \lambda_b$, the statistic $\mathcal{P}$ follows a uniform random law between 0 and 1, as shown in Figure 3. Therefore, one can easily test whether the computed value $\mathcal{P}$ for the specific case under investigation can be explained by the null hypothesis of 'no change' or not. For example, if we obtain $\mathcal{P} = 0.994$, then the probability that this value or a greater one could be obtained by chance if there was no change (null hypothesis) is $1 - 0.994 = 0.6\%$.

Marsan and Nalbant (2005) thus proposed to define the statistic γ as the log (in base 10) of the departure of $\mathcal{P}$ from 0.5:

$$\gamma \;=\; \log_{10} \mathcal{P} \tag{4}$$

if $\mathcal{P} < 0.5$, hence a decrease of activity, or

$$\gamma \;=\; -\; \log_{10}(1 - \mathcal{P}) \tag{5}$$

if $\mathcal{P} > 0.5$, hence an increase of activity. For example, if $\mathcal{P} = 10^{-3}$, then there is only a 10^{-3} chance that this apparent decrease or an even stronger one could be due to pure luck (null hypothesis of no change), and thus $\gamma = -3$. On the contrary, if $\mathcal{P} = 0.999 = 1 - 10^{-3}$, then the chance of observing this value or a greater one by chance is 10^{-3} also, and $\gamma = +3$. The statistic γ therefore provides an easy way

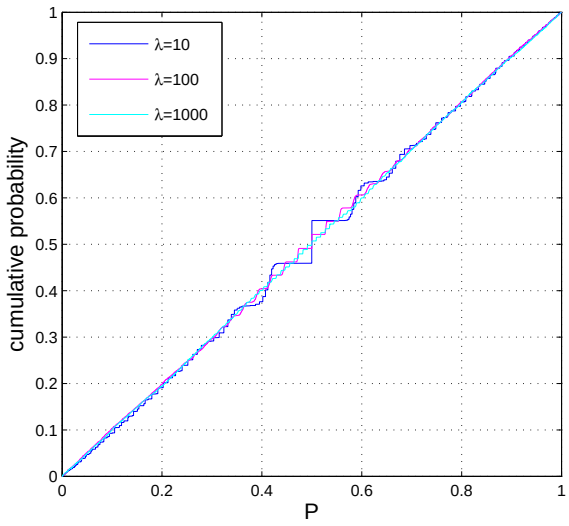

Fig. 3 Distribution of the probability $\mathcal{P}$ of an increase in seismicity rate, in the hypothesis of no change in rate. The two intervals *before* and *after* are characterized by the same rate λ, which takes three values as indicated on the graph. A unit time interval is considered for the two periods ($\Delta t_a = \Delta t_b = 1$). The distribution was obtained by running 10^4 independent simulations.

of telling whether we are close or far from respecting the no-change null hypothesis, and moreover gives the sign of the change. The value of γ can easily be interpreted in terms of a confidence level. For example, a confidence level of 95% corresponds to $\mathcal{P} < 0.025$ or $\mathcal{P} > 0.975$, hence a threshold value of $|\gamma| = 1.6$. Similarly, this threshold becomes $|\gamma| = 2.3$ for a confidence level of 99%.

This statistic is easy to implement:
(1) run `P=probability_increase(1,Nb,Na,Dtb,Dta);` cf above;
(2) compute γ as `gamma=-sign(P-0.5)*log(min([P 1-P]))/log(10);`

When Δt_a and Δt_b are different, the probability $\mathcal{P}$ departs from the uniform law for the null hypothesis of no change, as shown in Figure 4. However, this departure remains limited, the more so as the two durations are not too different, so that the statistic γ can still be used to a good approximation. Alternatively, γ can be computed by changing $\mathcal{P}$ into $-0.22\mathcal{P}^2 + 1.22\mathcal{P}$ if $\frac{\Delta t_a}{\Delta t_b} \gg 1$, or into $0.22\mathcal{P}^2 + 0.78\mathcal{P}$ if $\frac{\Delta t_a}{\Delta t_b} \ll 1$, cf. Figure 4.

As an example, if we consider the case of the Death Valley region, then $\mathcal{P} = 0.88$, cf. Table 2, and thus $\gamma = +0.92$, hence an increase which is not significant. On the contrary, for the Mono Basin region, $\mathcal{P} = 0.989$, thus $\gamma = +1.96$, which can be accepted as a significant rate change.

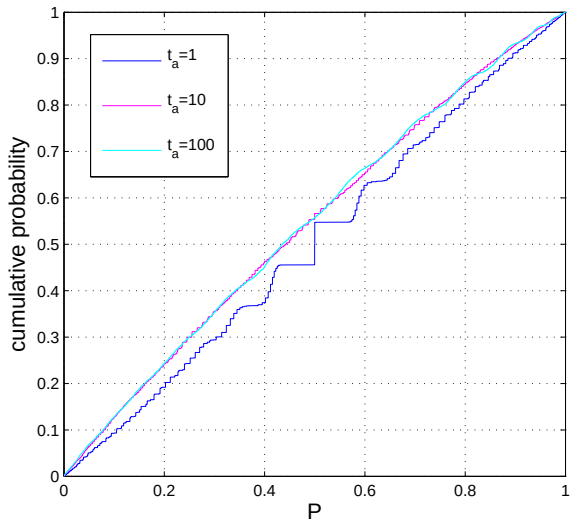

Fig. 4 Same as in Figure 3, but with $\Delta t_b = 1$ and a varying Δt_a as indicated on the graph. For $\Delta t_a \neq \Delta t_b$, the probability $\mathcal{P}$ slightly departs from a uniform law: a good fit of the cumulative probability is given by $Pr(\mathcal{P} < x) = -0.22x^2 + 1.22x$, for both $\Delta t_a = 10$ and $\Delta t_a = 100$.

4.2 Statistic β of *Matthews and Reasenberg* (1988)

Instead of considering the full probability densities as for example shown in Figure 1, one can compute the difference between the observed number N_a and the expected number $N_b \times \frac{\Delta t_a}{\Delta t_b}$, and rescale it by the typical dispersion (i.e., standard deviation) $\sqrt{N_b \times \frac{\Delta t_a}{\Delta t_b}}$. This gives the statistic

$$\beta = \frac{N_a - \Lambda}{\sqrt{\Lambda}} \tag{6}$$

$$\text{with } \Lambda = N_b \times \frac{\Delta t_a}{\Delta t_b} \tag{7}$$

Note that a symmetric measure could be proposed as $\frac{\Lambda - N_b}{\sqrt{\Lambda}}$ and $\Lambda = N_a \times \frac{\Delta t_b}{\Delta t_a}$, which is equal to β when $\Delta t_a = \Delta t_b$. For the Death Valley region, we obtain $\beta = +2.04$, while for the Mono Basin region $\beta = +5.19$. As can be seen with this example, large β values, sometimes greater (in absolute value) than 5, are needed to make sure the rate change is effectively significant. Such a large critical value is necessary here because the numbers N_b are small.

The translation of β into a probability can be done in the limit of large numbers of earthquake occurrences, for which the Poisson distribution tends to a Gaussian law. In the null hypothesis of no change, β is distributed like a Gaussian with zero

mean and unit standard deviation. Thus, for a positive β, the probability to obtain a greater value is $\frac{1}{2} - \frac{1}{2}\mathrm{erf}(\beta/\sqrt{2})$ where erf is the error function, while for a negative β the probability to obtain a smaller value is $\frac{1}{2} + \frac{1}{2}\mathrm{erf}(\beta/\sqrt{2})$.

It can be argued that, while being very simple to compute, the β-statistic is perhaps not the best choice: a symmetric version (as is the case of Z, cf. below) would be more appropriate, and the significance level of the rate change is not directly given by the value of β. Moreover, the underlying assumption of large numbers of earthquakes limits its use.

4.3 Statistic Z of *Habermann* (1981)

A measure was proposed by *Habermann* (1981) as

$$Z = \frac{N_a\ \Delta t_b\ -\ N_b\ \Delta t_a}{\sqrt{N_a\ \Delta t_b^2\ +\ N_b\ \Delta t_a^2}} \tag{8}$$

This is very similar to the β statistic, or, more exactly, is a symmetrical version of it, i.e., the denominator depending equally on both time intervals. As with the β statistic, in the limit of large numbers N_a and N_b, Z is distributed like a Gaussian law with zero mean and unit standard deviation, in the null hypothesis of no change. A derivation of this result can be found in *Marsan and Nalbant* (2005). Note that the original Z statistic as proposed by *Habermann* (1983) has the sign reversed from the one defined in Equation 8. We changed this sign to be coherent with the other statistical measures.

We compute Z for the Death Valley region: $Z = +1.21$, and for the Mono Basin region: $Z = +2.32$. The change can be considered as significant if $|Z| > 2$.

5 Accounting for nonstationary trends in earthquake activity

So far we have compared the observed N_a earthquakes after the time of interest T to the N_b occurrences before. The rationale of this comparison is that, if there were indeed no change, then we would expect N_a to be a random draw of the same Poisson process that generated N_b. However, this expectation must be reexamined if we know the earthquake activity is following a nonstationary trend at time T. The case of mainshock doublets or even multiplets is here particularly important: if we want to map the changes in seismicity (and thus of stress) brought by the second mainshock M_2, we first need to understand how the seismicity was evolving prior to it. Since the first mainshock M_1 initiated an aftershock sequence, this activity was likely to be decaying at the time of M_2. A model is therefore required to 'propagate'

the 'normal' aftershock activity of M_1 past the occurrence of M_2, so to compare between the observed earthquake rate and this predicted rate.

There are typically two ways to address the issue of nonstationarity. The more traditional method is to first decluster the dataset, which in principle should result in a stationary dataset for which the quantities described in Section 4 can then be applied. However, removing aftershocks from the earthquake catalog is in most cases not desirable. For example, testing whether a change in Coulomb stress caused by a mainshock implied a change in seismicity rate obviously requires to consider the aftershocks of this mainshock.

The other solution is to model the earthquake-generating process and its time evolution, knowing the history of the process up to time T, and then use this model to guess how λ_a should be distributed if there were no other change (apart from the 'normal' trend) at time T. This approach was developed in *Marsan* (2003). The main issue is to propose a good model that can well explain the evolution of the time series up to time T, and to extrapolate this time series between T and $T + t_a$.

As an example, Figure 5 extracted from *Daniel et al.* (2008) shows the case of the June 2000, Iceland, doublet, in which two very similar M_s6.6 vertical, strike-slip earthquakes occurred within 3.5 days and ∼15 km of each other. In this Figure, the seismicity rate at the Hengill triple junction (about 30 to 50 km away from the two earthquakes) is shown, after correction for completeness issues (white bars). Time 0 is 00:00, 17th of June, hence only a few hours before the occurrence of the first mainshock. This mainshock initiated an aftershock sequence in this zone, although we are far from the rupture zone itself. This sequence is modeled with an Omori-Utsu law; the fit is done from the time of the first mainshock to the time T of the second, and then extrapolated to $t > T$. A clear departure in seismicity rate from this trend just after the 2nd mainshock is observed, lasting for about 5 hours only. This increase in rate from the expected rate can then be tested using the various statistic described in Section 4.

The method for estimating rate changes in the context of nonstationary trends is then:

1. knowing earthquake activity up to time T, fit a model $\hat{\lambda}(t)$ to the seismicity rate;
2. extrapolate $\hat{\lambda}(t)$ to the time interval of duration Δt_a of interest;
3. deduce from this extrapolation a pdf $f(\lambda)$ for the expected λ for this interval. The simplest pdf is a Dirac $f(\lambda) = \delta(\lambda - \hat{\lambda})$ with its atom on the extrapolated value, but accounting for estimate uncertainties during the parameterization of the model $\hat{\lambda}(t)$, or even for the simple fact that in general the rate extrapolated over the whole interval Δt_a is not constant, would result in a more complex pdf;
4. use the statistic $\mathcal{P}$ and associated γ, with $f(\lambda)$ replacing $f_b(\lambda_b)$:

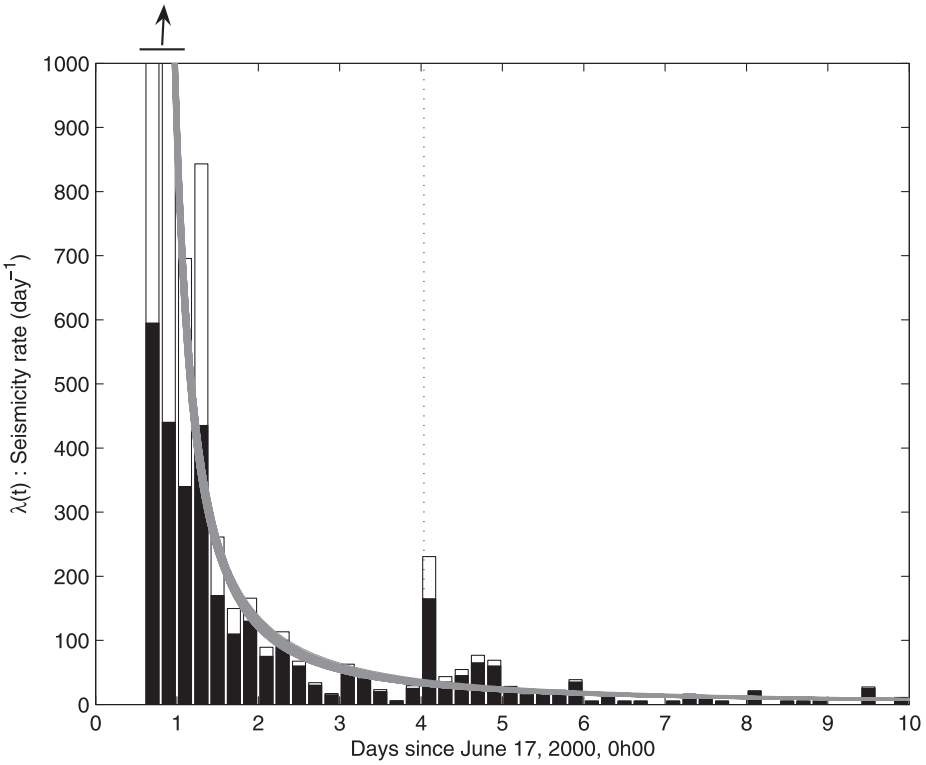

Fig. 5 Black bars: seismicity rates observed at Hengill Triple Junction frm 00:00 on June 17, 2000. The occurrence times of the two M_s6.6 mainshocks are indicated by the first bar and by the vertical dotted line, respectively. White bars: same as with the black bars, but after correcting for completeness issues. The rate is then for $m \geq 0$ earthquakes. Gray curve: best Omori-Utsu law fitted using the time interval between the two mainshock, that models the aftershock sequence in this zone caused by the first mainshock. It is further extrapolated after the second mainshock. Extracted from *Daniel et al.* (2008).

$$\mathcal{P} \;=\; 1 \;-\; \frac{1}{N_a!}\int_0^\infty dx\; f\left(\frac{x}{\Delta t_a}\right)\; \Gamma(N_a+1,x) \tag{9}$$

6 Searching for a significant change in the earthquake-generating process

In many applications, the rate change is estimated at a particular time T of interest, typically the occurrence of a mainshock. However, one can also be interested in checking whether there exists a significant change within a given interval, without a priori knowing the exact time T at which this change occurs. Then T is considered as an unknown parameter in this problem. Sophisticated methods have been proposed to address this problem (*Ogata* 1988, 1989, 1992, 1999, 2001), with a particular

emphasis on searching for anomalous seismicity rate decreases precursory to large shocks.

With this approach, one is interested in detecting the time at which the earthquake-generating process is significantly modified. To summarize, a model of seismicity is fitted to the data up to time T, and then extrapolated to later times $t > T$. Departure of the data at $t > T$ from this extrapolation is then sought for. An optimization is performed to maximize this departure, by changing the change-point T. Finally, for the optimized T, the significance of the departure between the data and the extrapolation is computed.

To illustrate this, and further detail the method, we discuss the case of the seismicity in the Aleutian arc from 1965 to 1989, taken from *Ogata* (1992), cf. Figure 6. In this analysis, a temporal ETAS model was fit to the data, separately for two distinct time intervals. The second time interval extends from some time in the year 1965 to 1975 (vertical dashed line in Figure 6). This model gives the expected earthquake rate $\hat{\lambda}(t)$ at any time t. Integrating this rate over time since a starting time T gives $\hat{\Lambda}(T,t) = \int_T^t ds\ \hat{\lambda}(s)$, the expected number of earthquakes that should have occurred, according to the model, between T and t.

If the model is good, then the actual number of earthquakes $N(T,t)$ between T and t should result from a Poisson process with mean rate 1 when considering the *transformed time* $\tau = \hat{\Lambda}(T,t)$ instead of the real time t. A plot of $N(T,t)$ vs. τ should thus show a curve close to a straight line of slope 1. Departure of $N(T,t)$ from this line therefore indicates that the model does not correctly explain the data. A measure can be proposed to test how significant this departure is (*Ogata* 1992):

$$\xi = \frac{N(T,t) - \hat{\Lambda}(T,t)}{\sqrt{\hat{\Lambda}(T,t) + \hat{\Lambda}(T,t)^2/N_0}} \tag{10}$$

where N_0 is the number of earthquakes that occurred in the fitting interval. The term related to N_0 in the denominator of Equation 10 is effectively a correction term that accounts for parameter uncertainties when fitting the model; such uncertainties are reduced when N_0 increases. Apart from this correction, ξ is very similar to the β statistic. Moreover, ξ is distributed like a Gaussian law with zero mean and unit standard deviation when the model well approximates the data. Optimization then amounts to find the best date for the changing-point T, so that the departure is the most significant.

A simpler approach to finding the best change-point date T is proposed in *Wyss and Habermann* (1988). It consists in computing the Z statistic for a varying time T, considering as *before* the earthquakes occurring between an initial time t_0 and T, and as *after* the earthquakes between T and an ending time t_1. The latter is typically the

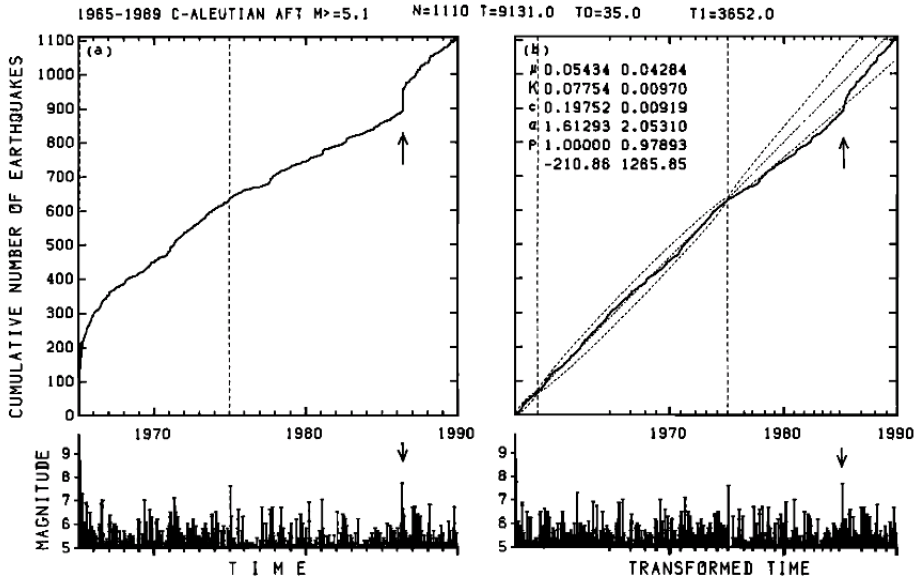

Fig. 6 Cumulative number of $m_b \geq 5.1$ earthquakes in the Aleutian arc (40^o < latitude < 80^o and 170^oE < longitude < 160^oW) from 1965 to 1989, vs. time (left) and vs. transformed time (right). The seismicity is modeled using a temporal ETAS model, with two set of parameters fitted over two distinct time intervals as shown with the vertical dashed lines (the first interval is all contained in 1965, year of the M_w8.7 great Rat Island earthquake). The model is then extrapolated past the second dashed line (year 1975) for constructing the transformed-time graph. On this graph, departure of the data from the central dotted curve past the lower-most dotted curve indicates a significant shutdown of activity, compared to what would have been predicted had the earthquake-generating process remained statistically the same after 1975. This relative quiescence lasts several year, up to the time of the 1986 M_s7.7 Andoreanof Islands earthquake (shown by the upward pointing arrow). Taken from *Ogata* (1992).

date of a large shock of interest, when searching for precursory quiescence patterns. The most significant Z is then selected. This first requires to decluster the data, as already mentioned when introducing the Z statistic.

Acknowledgements Many thanks to Katerina Orfanogiannaki and an anonymous reviewer for their constructive comments. D. M. benefited from financial support by ANR project ASEISMIC.

References

Daniel, G., D. Marsan, and M. Bouchon (2008), Earthquake triggering in southern iceland following the june 2000 ms 6.6 doublet, *J. Geophys. Res.*, *113*(B05310). 12, 13

Habermann, R. E. (1981), Precursory seismicity patterns: Stalking the mature seismic gap, in *Earthquake prediction - An international review*, edited by D. W. Simpson and P. G. Richards, pp. 29–42, American Geophysical Union. 11

Habermann, R. E. (1983), Teleseismic detection in the aleutian island arc, *J. Geophys. Res.*, *88*, 5056–5064. 11

Habermann, R. E. (1987), Man-made seismicity rate changes, *Bull. Seismol. S([0 3.5],A1*exp(alpha1*[0 3.5]),'k') oc. Am.*, *77*, 141–159. 4

Hill, D. P., P. A. Reasenberg, A. Michael, W. J. Arabaz, G. Beroza, D. Brumbaugh, J. N. Brune, R. Castro, S. Davis, D. dePolo, W. L. Ellsworth, J. Gomberg, S. Harmsen, L. House, S. M. Jackson, M. J. S. Johnston, L. Jones, R. Keller, S. Malone, L. Munguia, S. Nava, J. C. Pechmann, A. Sanford, R. W. Simpson, R. B. Smith, M. Stark, M. Stickney, A. Vidal, S. Walter, V. Wong, and J. Zollweg (1993), Seismicity remotely triggered by the magnitude 7.3 Landers, California, earthquake, *Science*, *260*(5114), 1617–1623. 4

Marsan, D. (2003), Triggering of seismicity at short time scales following californian earthquakes, *J. Geophys. Res.*, *108*, 2266. 12

Marsan, D., and S. S. Nalbant (2005), Methods for measuring seismicity rate changes: A review and a study of how the m-w 7.3 landers earthquake affected the aftershock sequence of the m-w 6.1 joshua tree earthquake, *Pageoph*, *162*(6-7), 1151–1185. 8, 11

Matthews, M. V., and P. A. Reasenberg (1988), Statistical methods for investigating quiescence and other temporal seismicity patterns, *Pageoph*, *126*, 357–372. 10

Ogata, Y. (1988), Statistical models for earthquake occurrences and residual analysis for point processes, *J. Am. Stat. Assoc.*, *83*(401), 9–27. 13

Ogata, Y. (1989), Statistical model for standard seismicity and detection of anomalies by residual analysis, *Tectonophys.*, *169*, 159–174. 13

Ogata, Y. (1992), Detection of precursory relative quiescence before great earthquakes trhough a statistical model, *J. Geophys. Res.*, *97*(B13), 19,845–19,871. 13, 14, 15

Ogata, Y. (1999), Seismicity analysis through point-process modeling: A review, *Pure Appl. Geophys.*, *155*, 471–507. 13

Ogata, Y. (2001), Increased probability of large earthquakes near aftershock regions with relative quiescence, *J. Geophys. Res.*, *106*(B5), 8729–8744. 13

Wyss, M., and R. E. Habermann (1988), Precursory quiescence before the august 1982 stone canyon, san andreas fault, earthquakes, *Pure Appl. Geophys.*, *126*(2-4), 334–356. 14